NASA/TM—2004-213438

Comparison of the Computational Efficiency of the Original Versus Reformulated High-Fidelity Generalized Method of Cells

Steven M. Arnold
Glenn Research Center, Cleveland, Ohio

Brett Bednarcyk
Ohio Aerospace Institute, Brook Park, Ohio

Jacob Aboudi
Tel Aviv University, Ramat Aviv, Israel

December 2004

The NASA STI Program Office . . . in Profile

Since its founding, NASA has been dedicated to the advancement of aeronautics and space science. The NASA Scientific and Technical Information (STI) Program Office plays a key part in helping NASA maintain this important role.

The NASA STI Program Office is operated by Langley Research Center, the Lead Center for NASA's scientific and technical information. The NASA STI Program Office provides access to the NASA STI Database, the largest collection of aeronautical and space science STI in the world. The Program Office is also NASA's institutional mechanism for disseminating the results of its research and development activities. These results are published by NASA in the NASA STI Report Series, which includes the following report types:

- TECHNICAL PUBLICATION. Reports of completed research or a major significant phase of research that present the results of NASA programs and include extensive data or theoretical analysis. Includes compilations of significant scientific and technical data and information deemed to be of continuing reference value. NASA's counterpart of peer-reviewed formal professional papers but has less stringent limitations on manuscript length and extent of graphic presentations.

- TECHNICAL MEMORANDUM. Scientific and technical findings that are preliminary or of specialized interest, e.g., quick release reports, working papers, and bibliographies that contain minimal annotation. Does not contain extensive analysis.

- CONTRACTOR REPORT. Scientific and technical findings by NASA-sponsored contractors and grantees.

- CONFERENCE PUBLICATION. Collected papers from scientific and technical conferences, symposia, seminars, or other meetings sponsored or cosponsored by NASA.

- SPECIAL PUBLICATION. Scientific, technical, or historical information from NASA programs, projects, and missions, often concerned with subjects having substantial public interest.

- TECHNICAL TRANSLATION. English-language translations of foreign scientific and technical material pertinent to NASA's mission.

Specialized services that complement the STI Program Office's diverse offerings include creating custom thesauri, building customized databases, organizing and publishing research results . . . even providing videos.

For more information about the NASA STI Program Office, see the following:

- Access the NASA STI Program Home Page at ***http://www.sti.nasa.gov***

- E-mail your question via the Internet to help@sti.nasa.gov

- Fax your question to the NASA Access Help Desk at 301–621–0134

- Telephone the NASA Access Help Desk at 301–621–0390

- Write to:
  NASA Access Help Desk
  NASA Center for AeroSpace Information
  7121 Standard Drive
  Hanover, MD 21076

NASA/TM—2004-213438

Comparison of the Computational Efficiency of the Original Versus Reformulated High-Fidelity Generalized Method of Cells

Steven M. Arnold
Glenn Research Center, Cleveland, Ohio

Brett Bednarcyk
Ohio Aerospace Institute, Brook Park, Ohio

Jacob Aboudi
Tel Aviv University, Ramat Aviv, Israel

National Aeronautics and
Space Administration

Glenn Research Center

December 2004

Available from

NASA Center for Aerospace Information
7121 Standard Drive
Hanover, MD 21076

National Technical Information Service
5285 Port Royal Road
Springfield, VA 22100

Available electronically at http://gltrs.grc.nasa.gov

Comparison of the Computational Efficiency of the Original Versus Reformulated High-Fidelity Generalized Method of Cells

Steven M. Arnold
National Aeronautics and Space Administration
Glenn Research Center
Cleveland, Ohio 44135 USA

Brett Bednarcyk
Ohio Aerospace Institute
Brook Park, Ohio 44142 USA

Jacob Aboudi
Tel Aviv University
Ramat Aviv 69978, Israel

Abstract

The High-Fidelity Generalized Method of Cells (HFGMC) micromechanics model has recently been reformulated by Bansal and Pindera (in the context of elastic phases with perfect bonding) to maximize its computational efficiency. This reformulated version of HFGMC has now been extended to include both inelastic phases and imperfect fiber-matrix bonding. The present paper presents an overview of the HFGMC theory in both its original and reformulated forms and a comparison of the results of the two implementations. The objective is to establish the correlation between the two HFGMC formulations and document the improved efficiency offered by the reformulation. The results compare the macro and micro scale predictions of the continuous reinforcement (doubly-periodic) and discontinuous reinforcement (triply-periodic) versions of both formulations into the inelastic regime, and, in the case of the discontinuous reinforcement version, with both perfect and weak interfacial bonding. The results demonstrate that identical predictions are obtained using either the original or reformulated implementations of HFGMC aside from small numerical differences in the inelastic regime due to the different implementation schemes used for the inelastic terms present in the two formulations. Finally, a direct comparison of execution times is presented for the original formulation and reformulation code implementations. It is shown that as the discretization employed in representing the composite repeating unit cell becomes increasingly refined (requiring a larger number of sub-volumes), the reformulated implementation becomes significantly (approximately an order of magnitude at best) more computationally efficient in both the continuous reinforcement (doubly-periodic) and discontinuous reinforcement (triply-periodic) cases.

1. Introduction

Micromechanical analyses provide the overall behavior of a multiphase material by taking into account the response of the individual constituents, their volume fractions and the detailed interaction between the phases. A review of various micromechanical models can be found in the monographs by Aboudi (1991) and Nemat-Nasser and Hori (1999) for example. In the present report, we discuss the computational efficiency of the recently reformulated high-fidelity generalized method of cells (HFGMC) micromechanical model. This model is the third generation in a sequence of micromechanical models; the first one being the method of cells (MOC) first described by Aboudi (1981) and used to model wave propagation in elastic fiber-reinforced composites. This work was followed by the prediction of the overall behavior of elastic-viscoplastic unidirectional composites using MOC, see Aboudi (1982). The use of the MOC to analyze various other types of composites appeared in several subsequent papers, all of which have been summarized in a monograph by Aboudi (1991). The number of different phases and

fiber architectures of a composite that the MOC was able to analyze was limited to four, thus motivating the advent of the generalized method of cells (GMC) theory (which forms the second generation in the sequence), put forth by Paley and Aboudi (1992), assuming continuous reinforcements and Aboudi (1995), assuming discontinuous reinforcements, which extended the model to an arbitrary number of phases with general architectures. This generalization extended the modeling capability of the MOC to include the following:

- Inelastic thermomechanical response of multiphase, e.g., metal matrix, composites.
- General modeling of composite architectures:
    1. Modeling of various fiber shapes by approximating the fiber-inclusion by a suitable assemblage of subcells.
    2. Analysis of different fiber array packing or distributions.
- Modeling of porosities and damage.
- Modeling of interfacial regions around inclusions, including interfacial degradation.

Two review papers documenting the application of MOC and GMC by various researchers has been presented by Aboudi (1996, 2004), respectively.

As discussed by Pindera and Bednarcyk (1999) for doubly-periodic composites and Bednarcyk and Pindera (2000) for triply-periodic composites, due to the inherent lack of shear coupling between normal and shear, stress and strain components within the GMC analysis, it is possible to dramatically reduce the order of the algebraic system by employing the subcell stresses as unknowns (instead of the strains). This efficient reformulation of the GMC yields a new system of algebraic equations, which is significantly smaller than the original (i.e., not reformulated) system, especially as the number of subcells increases. As a result of this reformulation of the GMC, the computational efficiency of the model is significantly improved. Consequently, the dramatic advantage of this reformulation is obvious, when one considers the analysis of inelastic composite structures, wherein the constitutive equations provided by the GMC are employed repeatedly at every integration point throughout the structure.

Although it has been extensively shown that GMC accurately predicts the macroscopic response of multiphase materials with periodic microstructures, both in the elastic and inelastic regions, the method's accuracy of estimating local stress and strain fields suffers in comparison to its macro predictive capability. This is rooted in the first-order representation of the displacement field in the individual phases and the satisfaction of the traction and displacement continuity conditions between the phases in a volume averaged sense. The net effect being the absence of so-called shear coupling, which ensures that both normal and shear stresses at the local level are present for a given macroscopically-applied stress. As a result, local stress fields are not well captured by the GMC; thus impacting the method's ability to predict accurately local events such as fiber and/or matrix damage evolution. This shortcoming has been corrected in the HFGMC theory (the now third generation of these micromechanics models) and was the driving motivation behind the development of this theory which is discussed in the next section.

Recently, NASA Glenn Research Center, in conjunction with its partners, has developed a micromechanics analysis code (based on aforementioned generalized method of cells toolset) known as MAC/GMC, which has many user friendly features and significant flexibility for the analysis of continuous, discontinuous, laminate, or woven (polymeric, ceramic, and/or metal matrix) composites with phases that can be represented by arbitrary elastic, viscoelastic, and/or viscoplastic constitutive models. The most recent version of this code (Version 4, see Bednarcyk and Arnold (2002a)) incorporates not only GMC but HFGMC as well, along with additional material models including smart (electromagnetic and shape memory alloy) materials, and yield surface prediction for metal matrix composites.

2. The High-Fidelity Generalized Method of Cells (HFGMC)

The HFGMC discussed herein is an extension/specialization of the linear electro-magneto-thermo-elastic triply-periodic theory for discontinuously reinforced, (i.e., short-fiber), composites described by Aboudi (2001), to that of thermoinelastic behavior of composites with discontinuous weakly

bonded fibers. The inclusion of inelastic phases follows the analysis that has been presented previously by Aboudi et al. (2002, 2003) for the case of continuous fibers, i.e. doubly-periodic boundary conditions. In the present paper, this micromechanical model will be briefly outlined with special attention paid to describing the inelastic and imperfect bonding extensions.

The model is based on a homogenization technique for composites with triply-periodic microstructure (for example, those representative of discontinuously reinforced composites), where figure 1a shows this periodic microstructure in the global $\boldsymbol{x}$ coordinate system. The parallelepiped repeating unit cell (RUC) illustrated in figure 1(b), defined with respect to RUC coordinates (y_1, y_2, y_3), of such a composite is divided into N_α, N_β, and N_γ subcells in the y_1, y_2, and y_3 directions, respectively. Each subcell (illustrated in figure 1c) is identified by the indices ($\alpha\beta\gamma$) with $\alpha = 1,\ldots, N_\alpha$, $\beta = 1,\ldots, N_\beta$, and $\gamma = 1,\ldots, N_\gamma$, and may contain a distinct homogeneous material. The dimensions of the subcell are denoted by d_α, h_β, and l_γ, respectively. A local coordinate system, ($\overline{y}_1^{(\alpha)}$, $\overline{y}_2^{(\beta)}$, $\overline{y}_3^{(\gamma)}$) is introduced in each subcell whose origin is located at its center, see figure 1c. The local (subcell) constitutive equation of the material which, in general, is assumed to be thermoinelastic is given by

$$\boldsymbol{\sigma}^{(\alpha\beta\gamma)} = \mathbf{C}^{(\alpha\beta\gamma)}\left(\boldsymbol{\varepsilon}^{(\alpha\beta\gamma)} - \boldsymbol{\varepsilon}^{I(\alpha\beta\gamma)}\right) - \boldsymbol{\Gamma}^{(\alpha\beta\gamma)}\Delta T \tag{1}$$

where $\boldsymbol{\sigma}^{(\alpha\beta\gamma)}$, $\boldsymbol{\varepsilon}^{(\alpha\beta\gamma)}$, $\boldsymbol{\varepsilon}^{I(\alpha\beta\gamma)}$, and $\boldsymbol{\Gamma}^{(\alpha\beta\gamma)}$ are the stress, total strain, inelastic strain and thermal stress tensors, respectively, in subcell ($\alpha\beta\gamma$). In eq. (1), $\mathbf{C}^{(\alpha\beta\gamma)}$ is the elastic stiffness tensor of the material for subcell ($\alpha\beta\gamma$), and ΔT denotes the temperature deviation from a reference temperature. Lastly, the inelastic strain $\boldsymbol{\varepsilon}^{I(\alpha\beta\gamma)}$ can be obtained from either a Prandtl-Reuss classical plasticity formulation (Mendelson (1986)) or by an appropriate integration of a viscoplastic formulation (i.e., set of flow and evolution equations) for example.

The basic assumption in HFGMC is that the displacement vector $\mathbf{u}^{(\alpha\beta\gamma)}$ in each subcell is expanded into quadratic form[1] in terms of its local coordinates ($\overline{y}_1^{(\alpha)}$, $\overline{y}_2^{(\beta)}$, $\overline{y}_3^{(\gamma)}$) as follows:

$$\begin{aligned}\mathbf{u}^{(\alpha\beta\gamma)} = \overline{\boldsymbol{\varepsilon}}\,\mathbf{x} + \mathbf{W}_{(000)}^{(\alpha\beta\gamma)} + \overline{y}_1^{(\alpha)}\mathbf{W}_{(100)}^{(\alpha\beta\gamma)} + \overline{y}_2^{(\beta)}\mathbf{W}_{(010)}^{(\alpha\beta\gamma)} + \overline{y}_3^{(\gamma)}\mathbf{W}_{(001)}^{(\alpha\beta\gamma)} + \frac{1}{2}\left(3\overline{y}_1^{(\alpha)2} - \frac{d_\alpha^2}{4}\right)\mathbf{W}_{(200)}^{(\alpha\beta\gamma)} \\ + \frac{1}{2}\left(3\overline{y}_2^{(\beta)2} - \frac{h_\beta^2}{4}\right)\mathbf{W}_{(020)}^{(\alpha\beta\gamma)} + \frac{1}{2}\left(3\overline{y}_3^{(\gamma)2} - \frac{l_\gamma^2}{4}\right)\mathbf{W}_{(002)}^{(\alpha\beta\gamma)}\end{aligned} \tag{2}$$

where $\overline{\boldsymbol{\varepsilon}}$ is the applied (external) average strain tensor, $\mathbf{x}$ is the global coordinate vector (see fig. 1a), and the unknown terms $\mathbf{W}_{(lmn)}^{(\alpha\beta\gamma)}$, must be determined from the fulfillment of the equilibrium conditions, the periodic boundary conditions, and the interfacial continuity conditions of displacements and tractions between subcells. The periodic boundary conditions ensure that the displacements and tractions at opposite surfaces of the repeating unit cell are identical, see Aboudi (2001) for more details. A foundational assumption in the present micromechanical analysis is that all these conditions are imposed in an average (integral) sense.

[1] It should be mentioned that both MOC and GMC employ a first order expansion of the displacement vector in each subcell. Furthermore, the present second order (quadratic) expansion, eq. (2), that is foundational to the HFGMC theory has been previously employed by Aboudi (1986, 1987, 1988) in the analysis of wave propagation in composite materials, and by Aboudi et al. (1999) in the determination of the response of functionally graded materials to thermoelastic loading.

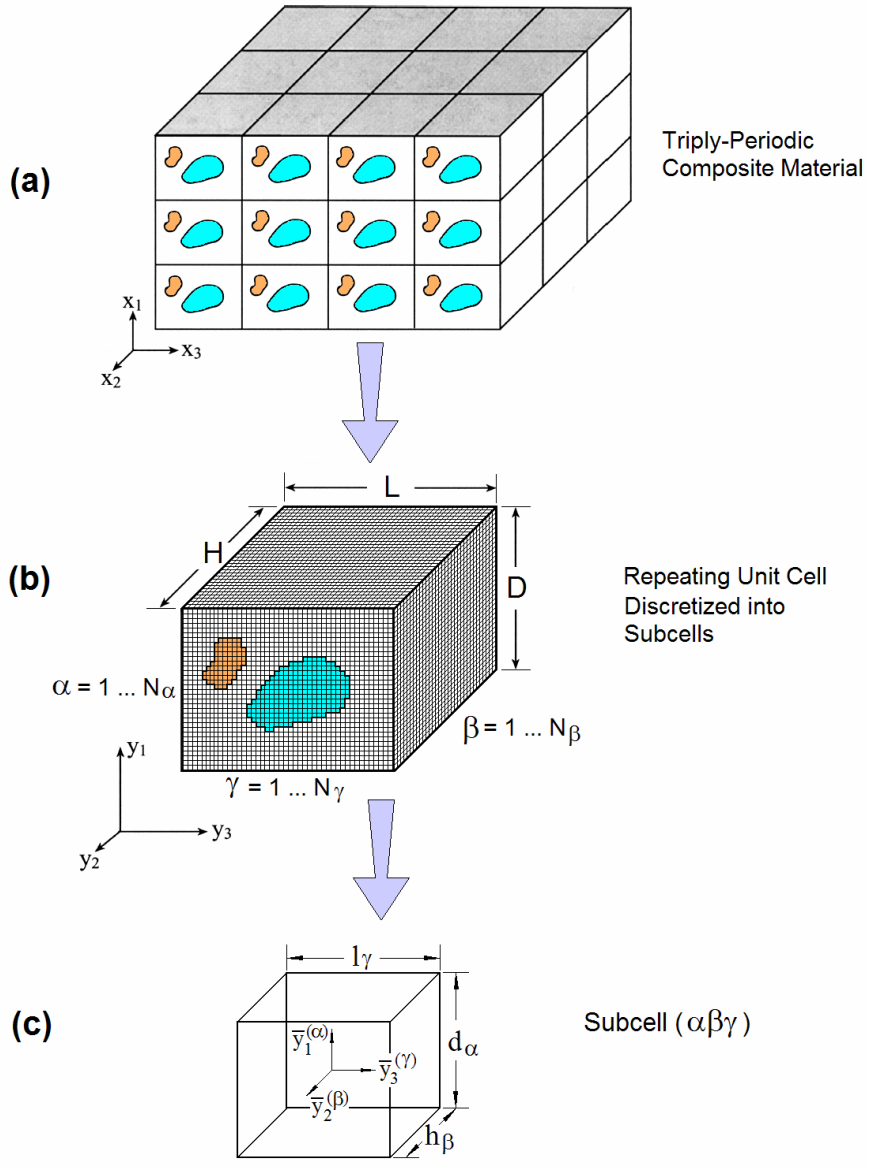

Figure 1.—(a) A multiphase composite with triply-periodic microstructure. (b) The repeating unit cell, defined in the (y_1, y_2, y_3) coordinate system, is discretized into $N_\alpha \times N_\beta \times N_\gamma$ subcells. (c) The monolithic subcell is defined in the local coordinate system ($\overline{y}_1^{(\alpha)}$, $\overline{y}_2^{(\beta)}$, $\overline{y}_3^{(\gamma)}$).

Consequently, imposition of the equilibrium equations in each subcell together with the application of the interfacial and periodicity conditions results in a linear system of algebraic equations being obtained which can be represented in the following form:

$$\mathbf{KU} = \mathbf{f} + \mathbf{g} \tag{3}$$

where the matrix **K** contains information on the geometry and thermomechanical properties of the materials within the individual subcells ($\alpha\beta\gamma$), and the displacement vector **U** contains the unknown displacement coefficients $\mathbf{W}_{(lmn)}^{(\alpha\beta\gamma)}$ which appear on the right-hand side of eq. (2). The thermomechanical vector **f** contains information on the applied average strains $\overline{\boldsymbol{\varepsilon}}$ and the imposed temperature deviation ΔT; while the inelastic force vector **g** appearing on the right-hand side of eq. (3) contains the inelastic effects given in terms of the integrals of the inelastic strain distributions. Note, the inelastic integrals within **g** depend implicitly on the elements of the displacement coefficient vector **U**, thus requiring an incremental solution of eq. (3) at each point along the loading path, see Aboudi et al. (2003) for more details.

The solution of eq. (3) then enables the establishment of the following localization relation which relates the average strain $\overline{\boldsymbol{\varepsilon}}^{(\alpha\beta\gamma)}$ in the subcell ($\alpha\beta\gamma$) to the externally applied average $\overline{\boldsymbol{\varepsilon}}$ in the form:

$$\overline{\boldsymbol{\varepsilon}}^{(\alpha\beta\gamma)} = \mathbf{A}^{(\alpha\beta\gamma)}\overline{\boldsymbol{\varepsilon}} + \mathbf{A}^{th(\alpha\beta\gamma)}\Delta T + \mathbf{D}^{I(\alpha\beta\gamma)} \tag{4}$$

where $\mathbf{A}^{(\alpha\beta\gamma)}$ and $\mathbf{A}^{th(\alpha\beta\gamma)}$ are the mechanical and thermal strain concentration tensors, respectively, of the subcell ($\alpha\beta\gamma$), and $\mathbf{D}^{I(\alpha\beta\gamma)}$ is a vector that involves the current inelastic effects in the subcell (see Aboudi, 2004).

The final form of the effective constitutive law of the multiphase thermo-inelastic composite, which relates the average (macro) stress $\overline{\boldsymbol{\sigma}}$ and strain $\overline{\boldsymbol{\varepsilon}}$, is established as follows:

$$\overline{\boldsymbol{\sigma}} = \mathbf{C}^{*}\,\overline{\boldsymbol{\varepsilon}} - \left(\boldsymbol{\Gamma}^{*}\Delta T + \overline{\boldsymbol{\sigma}}^{I}\right) \tag{5}$$

In this equation $\mathbf{C}^{*}$ is the effective elastic stiffness tensor, $\boldsymbol{\Gamma}^{*}$ is the effective thermal stress tensor of the composite, and $\overline{\boldsymbol{\sigma}}^{I}$ is the global inelastic stress tensor. All of these global quantities can be expressed in a closed-form manner in terms of the mechanical and thermal concentration tensors which appear in eq. (4) together with the inelastic term $\mathbf{D}^{I(\alpha\beta\gamma)}$, see Aboudi et al. (2001, 2002, 2003) and Aboudi (2004) for more details. They are given as follows:

$$\mathbf{C}^{*} = \frac{1}{DHL}\sum_{\alpha=1}^{N_\alpha}\sum_{\beta=1}^{N_\beta}\sum_{\gamma=1}^{N_\gamma} d_\alpha h_\beta l_\gamma \mathbf{C}^{(\alpha\beta\gamma)}\mathbf{A}^{(\alpha\beta\gamma)} \tag{6}$$

$$\boldsymbol{\Gamma}^{*} = \frac{-1}{DHL}\sum_{\alpha=1}^{N_\alpha}\sum_{\beta=1}^{N_\beta}\sum_{\gamma=1}^{N_\gamma} d_\alpha h_\beta l_\gamma \left[\mathbf{C}^{(\alpha\beta\gamma)}\mathbf{A}^{th(\alpha\beta\gamma)} - \boldsymbol{\Gamma}^{(\alpha\beta\gamma)}\right] \tag{7}$$

$$\overline{\boldsymbol{\sigma}}^{I} = \frac{-1}{DHL}\sum_{\alpha=1}^{N_\alpha}\sum_{\beta=1}^{N_\beta}\sum_{\gamma=1}^{N_\gamma} d_\alpha h_\beta l_\gamma \left[\mathbf{C}^{(\alpha\beta\gamma)}\mathbf{D}^{I(\alpha\beta\gamma)} - \mathbf{R}_{(0,0,0)}^{(\alpha\beta\gamma)}\right] \tag{8}$$

where $\mathbf{R}_{(0,0,0)}^{(\alpha\beta\gamma)}$ is an expression that represents the integral of the inelastic strain distributions and *D*, *H*, and *L* are the repeating unit cell dimensions (see fig. 1b).

Equation (3) forms a system of $21N_\alpha N_\beta N_\gamma$ algebraic equations. The size of this matrix (and thus the solution time) can however, be significantly reduced by utilizing the continuity of displacements

across the interfaces between the phases in the case of perfect bonding. This reformulation of HFGMC for computational speed was originally[2] put forth by Bansal and Pindera (2004) for the special case of continuous, perfectly bonded fibers (i.e., doubly-periodic case) and linear elasticity. Therein the number of unknowns is shown to be reduced (by approximately half when compared to the original) by treating the average displacements at the surfaces of the subcells as the only unknowns. In the present case of discontinuous fibers (i.e., the triply-periodic case) the same concept will be applied wherein the average displacement at the surface $\overline{y}_1^{(\alpha)} = -d_\alpha/2$ of subcell $(\alpha\beta\gamma)$ is given by:

$$\overset{(1)}{\overline{\mathbf{u}}}{}^{(\alpha\beta\gamma)} = \frac{1}{h_\beta l_\gamma} \int_{-h_\beta/2}^{h_\beta/2} \int_{-l_\gamma/2}^{l_\gamma/2} \left[\mathbf{u}^{(\alpha\beta\gamma)} \Big|_{\overline{y}_1^{(\alpha)} = -\frac{d_\alpha}{2}} \right] d\overline{y}_2^{(\beta)}\, d\overline{y}_3^{(\gamma)} \tag{9}$$

with similar definitions of the average surface displacements $\overset{(2)}{\overline{\mathbf{u}}}{}^{(\alpha\beta\gamma)}$ and $\overset{(3)}{\overline{\mathbf{u}}}{}^{(\alpha\beta\gamma)}$ evaluated at the surfaces $\overline{y}_2^{(\beta)} = -h_\beta/2$ and $\overline{y}_3^{(\gamma)} = -l_\gamma/2$, respectively, of this subcell. It should be emphasized that the introduction of the average surface displacements at $\overline{y}_1^{(\alpha)} = d_\alpha/2$, $\overline{y}_2^{(\beta)} = h_\beta/2$, and $\overline{y}_3^{(\gamma)} = l_\gamma/2$ is not necessary because these displacements are equal, due to the interfacial continuity, to $\overset{(1)}{\overline{\mathbf{u}}}{}^{(\alpha+1,\beta,\gamma)}$, $\overset{(2)}{\overline{\mathbf{u}}}{}^{(\alpha,\beta+1,\gamma)}$, and $\overset{(3)}{\overline{\mathbf{u}}}{}^{(\alpha,\beta,\gamma+1)}$, respectively. Consequently in terms of these average surface displacements in all subcells, the new system of equations that replaces eq. (3) in the efficient reformulation of HFGMC is given by

$$\mathbf{K}'\overline{\mathbf{U}} = \mathbf{f}' + \mathbf{g}' \tag{10}$$

where, as in eq. (3), the matrix $\mathbf{K}'$ contains information on the geometry and thermomechanical properties of the materials within the individual subcells $(\alpha\beta\gamma)$, and the vector $\overline{\mathbf{U}}$ contains the unknown average surface displacements of all subcells. The latter can be related to the unknown field quantities $\mathbf{W}_{(lmn)}^{(\alpha\beta\gamma)}$ which appear on the right-hand side of eq. (2). Here too, the mechanical vector $\mathbf{f}'$ contains information on the applied average strains $\overline{\boldsymbol{\varepsilon}}$ and the imposed temperature deviation ΔT. The inelastic force vector $\mathbf{g}'$ appearing on the right-hand side of eq. (10) contains the inelastic effects given in terms of the integrals of the inelastic strain distributions. As a result of this reformulation (where the unknowns now are only the average surface displacements) the size of the system of algebraic equations, see eq. (10), becomes: $9N_\alpha N_\beta N_\gamma + 3\left(N_\alpha N_\beta + N_\alpha N_\gamma + N_\beta N_\gamma\right)$ as compared to the previous original formulation with $21N_\alpha N_\beta N_\gamma$ unknowns. A comparison of the number of unknowns present in both the doubly-periodic and triply-periodic versions of the original formulation and reformulation of HFGMC is plotted in figure 2. Clearly, since the solution speed for the inversion of a given system of equations is on the order of the rank cubed of the matrix, it is immediately obvious that in the limit, i.e., $(21/9)^3$, this reformulation could enhance the solution speed by approximately a factor of 12 at best. In the case of sparse solvers this rank cubed relation is not completely applicable as additional matrix characteristics come into play.

[2] Note, Zhong and Pindera (2002) and Bansal and Pindera (2002, 2003) earlier proposed an equivalent reformulation (i.e., reduction in variable formulation) for HFGMC's non-periodic, predecessor—HOTFGM (Higher Order Theory for Functionally Graded Materials).

Note that comparing the number of unknowns required by HFGMC (original/reformulated) to its corresponding predecessor GMC (original/reformulated) it becomes obvious that in the limit the original HFGMC formulation (HFGMC/GMC = $21N^3/6N^3$, assuming $N_\alpha = N_\beta = N_\gamma = N$) has 3.5 times more unknowns than does GMC, whereas in the case of the reformulation, the ratio is

$$\lim_{N\to\infty}\left(\frac{9N^3+9N^2}{3N^2+3N}\right)=3N$$

Therefore, again assuming the use of a classic approach for inverting the matrix, this would mean that GMC original is approximately 43 times faster than HFGMC original; however comparing reformulated GMC to HFGMC we see that GMC's maximum speed-up as compared with HFGMC is $27N^3$. For example, given a 12×12×12, repeating unit cell, the maximum reformulated speed-up ratio indicates that if a solution using HFGMC would take approximately 13 hours then GMC would take approximately 1 second. Consequently, even though GMC does not predict local fields as accurately as does HFGMC it still provides similar global accuracy as compared with HFGMC, thus it remains a valuable tool in the formulation of a multiscale computational approach.

Thus far perfect bonding has been assumed to exist at the interfaces between subcells such that the displacements are continuous across any interface. The generalization of HFGMC to the case of imperfect bonding between phases has been presented previously by Bednarcyk et al. (2004) for the case of continuous fibers. There and herein the debonding model utilized follows that of Bednarcyk and Arnold (2000, 2002b), that is:

$$\left[u_j\right]^{Int} = R_j\left(t\right)t_j\Big|^{Int} \tag{11}$$

where $\left[u_j\right]^{Int}$ is the discontinuity in displacement component j at interface Int, $t_j\Big|^{Int}$ is the corresponding traction component at interface Int, and $R_j\left(t\right)$ is a time-dependent proportionality function. The introduction of such a debonding model, as given by eq. (11), requires a somewhat different and more complicated mathematical derivation to accomplish the efficient reformulation of HFGMC. This is because; now the continuity of displacement at the interfaces between subcells is no longer valid and now requires the utilization of eq. (11) instead of the procedure described by eqs. (9) and (10).

The major steps illustrating how this reformulation can be achieved in the presence of imperfect bonding between the phases is briefly outlined below, with further details reserved for a later publication. Let us temporarily introduce the average displacements at the interfaces evaluated at $\overline{y}_1^{(\alpha)} = d_\alpha/2$, $\overline{y}_2^{(\beta)} = h_\beta/2$, and $\overline{y}_3^{(\gamma)} = l_\gamma/2$ which are denoted, respectively, by: $\overset{(1)+}{\mathbf{u}}{}^{(\alpha\beta\gamma)}$, $\overset{(2)+}{\mathbf{u}}{}^{(\alpha\beta\gamma)}$, and $\overset{(3)+}{\mathbf{u}}{}^{(\alpha\beta\gamma)}$. For example,

$$\overset{(1)+}{\mathbf{u}}{}^{(\alpha\beta\gamma)} = \frac{1}{h_\beta\, l_\gamma}\int_{-h_\beta/2}^{h_\beta/2}\int_{-l_\gamma/2}^{l_\gamma/2}\left[\mathbf{u}^{(\alpha\beta\gamma)}\Big|_{\overline{y}_1^{(\alpha)}=\frac{d_\alpha}{2}}\right]d\overline{y}_2^{(\beta)}\,d\overline{y}_3^{(\gamma)} \tag{12}$$

These variables are not needed in the reformulation analysis neither in the perfect bonding case (as stated before) nor in the imperfect case, yet are merely introduced here as an intermediate stage to aid in explanation.

By implementing eq. (11) and evaluating it in the average sense at the surface whose normal is in the 1-direction at $\overline{y}_1^{(\alpha)} = d_\alpha/2$, one obtains the expression:

$$\overset{(1)+}{\mathbf{u}}{}^{(\alpha\beta\gamma)} = \overset{(1)}{\overline{\mathbf{u}}}{}^{(\alpha+1,\beta,\gamma)} - \mathbf{R}^{(\alpha)}(t)\,\overset{(1)+}{\mathbf{t}}{}^{(\alpha\beta\gamma)} \tag{13}$$

where $\overset{(1)+}{\mathbf{t}}{}^{(\alpha\beta\gamma)}$ is the surface average of the traction vector evaluated at $\overline{y}_1^{(\alpha)} = d_\alpha/2$, namely

$$\overset{(1)+}{\mathbf{t}}{}^{(\alpha\beta\gamma)} = \frac{1}{h_\beta\, l_\gamma} \int_{-h_\beta/2}^{h_\beta/2} \int_{-l_\gamma/2}^{l_\gamma/2} \mathbf{t}^{(\alpha\beta\gamma)}\Big|_{\overline{y}_1^{(\alpha)} = \frac{d_\alpha}{2}} d\overline{y}_2^{(\beta)}\, d\overline{y}_3^{(\gamma)} \tag{14}$$

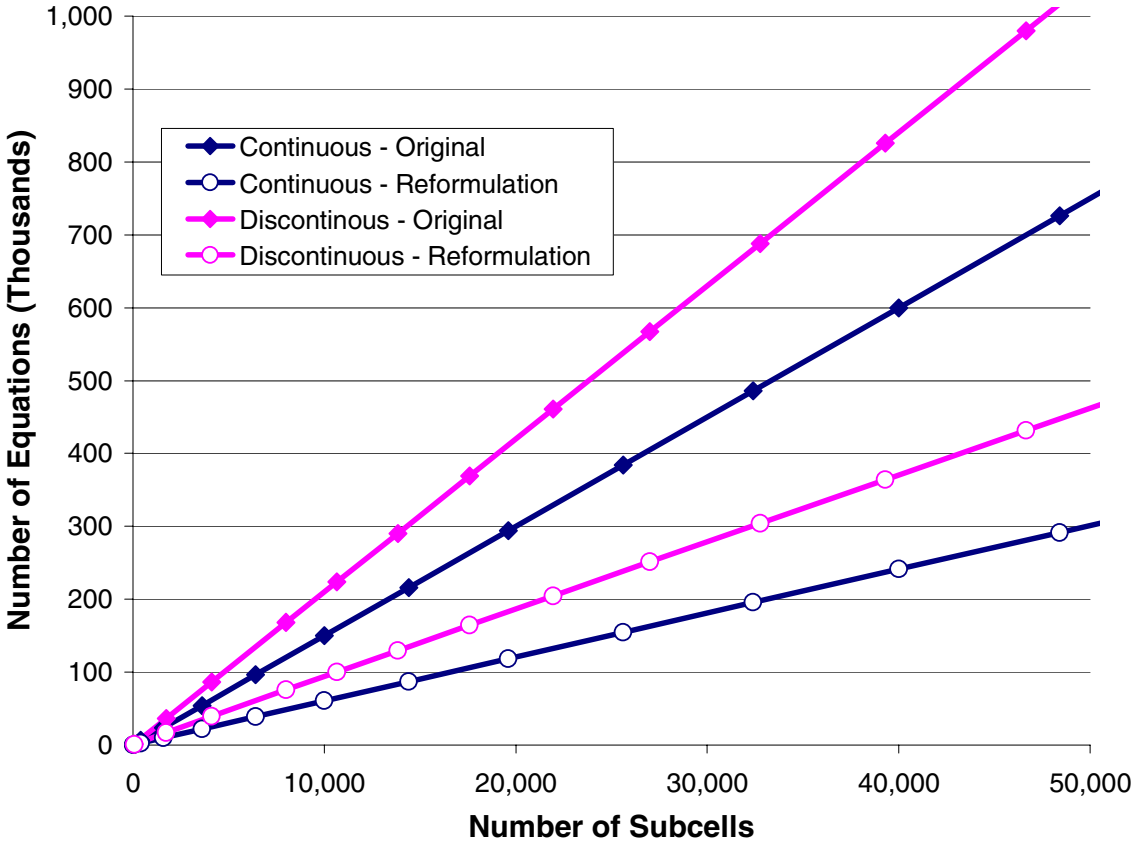

Figure 2.—Plot of number of unknowns vs. number of subcells (assuming an equal number of subcells in each direction) for the original and reformulated versions of the doubly-periodic and triply-periodic HFGMC.

and $\mathbf{R}^{(\alpha)}(t)$ is a vector that denotes the appropriate debonding time-dependent parameters at this surface.

Similar to eq. (13), we obtain by averaging over the other two surfaces at $\overline{y}_2^{(\beta)} = h_\beta/2$ and $\overline{y}_3^{(\gamma)} = l_\gamma/2$ that

$$\overset{(2)+}{\mathbf{u}}{}^{(\alpha\beta\gamma)} = \overset{(2)}{\overline{\mathbf{u}}}{}^{(\alpha,\beta+1,\gamma)} - \mathbf{R}^{(\beta)}(t)\,\overset{(2)+}{\mathbf{t}}{}^{(\alpha\beta\gamma)} \tag{15}$$

$$\overset{(3)+}{\mathbf{u}}{}^{(\alpha\beta\gamma)} = \overset{(3)}{\overline{\mathbf{u}}}{}^{(\alpha,\beta,\gamma+1)} - \mathbf{R}^{(\gamma)}(t)\,\overset{(3)+}{\mathbf{t}}{}^{(\alpha\beta\gamma)} \tag{16}$$

One can immediately observe from eqs. (13), (15), and (16) that unlike in the perfect bonding case where $\overset{(1)+}{\mathbf{u}}{}^{(\alpha\beta\gamma)} = \overset{(1)}{\overline{\mathbf{u}}}{}^{(\alpha+1,\beta,\gamma)}$, $\overset{(2)+}{\mathbf{u}}{}^{(\alpha\beta\gamma)} = \overset{(2)}{\overline{\mathbf{u}}}{}^{(\alpha,\beta+1,\gamma)}$, and $\overset{(3)+}{\mathbf{u}}{}^{(\alpha\beta\gamma)} = \overset{(3)}{\overline{\mathbf{u}}}{}^{(\alpha,\beta,\gamma+1)}$, these quantities (denoted by '+') are related to the corresponding adjacent average surface displacements (denoted by 'bar') in a complicated manner that involves both the average surface tractions and the debonding parameters. By employing the constitutive equations of the material that occupies the subcell ($\alpha\beta\gamma$), these surface tractions can be immediately related to the surface displacements $\overset{(1)+}{\mathbf{u}}{}^{(\alpha\beta\gamma)}$, $\overset{(1)}{\overline{\mathbf{u}}}{}^{(\alpha\beta\gamma)}$, $\overset{(2)+}{\mathbf{u}}{}^{(\alpha\beta\gamma)}$, $\overset{(2)}{\overline{\mathbf{u}}}{}^{(\alpha\beta\gamma)}$, $\overset{(3)+}{\mathbf{u}}{}^{(\alpha\beta\gamma)}$, and $\overset{(3)}{\overline{\mathbf{u}}}{}^{(\alpha\beta\gamma)}$. Consequently, we can rewrite eqs. (13), (15), and (16) by moving all quantities with the '+' superscript to the left-hand side, while keeping all 'bar' quantities as well as the thermal and inelastic variables on the right-hand side. Thus eqs. (13), (15), and (16) provide us with a system of nine algebraic equations that relate the nine variables: $\overset{(1)+}{\mathbf{u}}{}^{(\alpha\beta\gamma)}$, $\overset{(2)+}{\mathbf{u}}{}^{(\alpha\beta\gamma)}$, $\overset{(3)+}{\mathbf{u}}{}^{(\alpha\beta\gamma)}$ to $\overset{(1)}{\overline{\mathbf{u}}}{}^{(\alpha+1,\beta,\gamma)}$, $\overset{(1)}{\overline{\mathbf{u}}}{}^{(\alpha\beta\gamma)}$, $\overset{(2)}{\overline{\mathbf{u}}}{}^{(\alpha,\beta+1,\gamma)}$, $\overset{(2)}{\overline{\mathbf{u}}}{}^{(\alpha\beta\gamma)}$, $\overset{(3)}{\overline{\mathbf{u}}}{}^{(\alpha,\beta,\gamma+1)}$, and $\overset{(3)}{\overline{\mathbf{u}}}{}^{(\alpha\beta\gamma)}$. Let us represent this system of nine equations by:

$$\mathbf{F}\mathbf{U}^{+} = \mathbf{H}\overline{\mathbf{U}} + \textit{thermoinelastic terms} \tag{17}$$

where $\mathbf{F}$ and $\mathbf{H}$ are matrices whose elements depend on the material properties and geometry of the material within the subcell as well as the debonding parameters that characterize its surfaces. The formal solution of this system of equations provides the requested relations between $\mathbf{U}^{+}$ and $\overline{\mathbf{U}}$, i.e.:

$$\mathbf{U}^{+} = \mathbf{F}^{-1}\left[\mathbf{H}\overline{\mathbf{U}} + \textit{thermoinelastic terms}\right] \tag{18}$$

In conclusion, unlike the perfect bonding case where $\mathbf{U}^{+}$ is immediately related to $\overline{\mathbf{U}}$, in the case of weak bonding this relation is given in terms of $\overline{\mathbf{U}}$ by lengthy and somewhat complicated expressions (as a result of which the coding is presently far more complicated). In both cases the variables $\mathbf{U}^{+}$ are not

needed or used in the programming and thus the number of unknowns in eq. (10) in the imperfect bonding and the perfect bonding cases is the same (namely, $9N_\alpha N_\beta N_\gamma + 3\left(N_\alpha N_\beta + N_\alpha N_\gamma + N_\beta N_\gamma\right)$).

3. Results and Discussion

The results presented herein serve two purposes. First, they establish the correlation between the predictive capabilities of the original and reformulated versions of HFGMC, in both the elastic and inelastic regimes. Second, they document the improved computational efficiency offered by the efficient reformulation. Both the continuously reinforced (doubly-periodic) and discontinuously reinforced (triply-periodic) versions of HFGMC will be employed to model a 25% boron/aluminum (B/Al) material system. These two classes of problems merely constitute specializations of the more general capability present in the fully coupled thermo-electro-magneto-mechanical reformulated HFGMC code. The isotropic boron fiber (inclusion) is considered to be isotropic and elastic, while the aluminum matrix is considered to be isotropic and elasto-plastic. Mendelson's (1986) incremental plasticity theory is employed to model the inelastic aluminum matrix response (see Aboudi et al., 2003 for details). For the demonstration results presented herein, the aluminum matrix is treated as elastic-perfectly plastic (i.e., with no inelastic hardening). The material properties for the boron and aluminum materials are given in table 1.

For the continuously reinforced (doubly-periodic) composite case, the employed RUC is shown in figure 3, where the RUC has been discretized into 32×32 subcells so as to capture the circular geometry of the fiber cross-section sufficiently. This RUC was employed to simulate the longitudinal (in the fiber direction) and transverse tensile response of a 25% B/Al composite (assuming perfect fiber-matrix bonding), with the predicted global responses being shown in figure 4. As expected, the composite is considerably stiffer in the longitudinal direction compared to the transverse and matrix plasticity is also much more pronounced in the transverse direction. Clearly, figure 4 indicates that the global responses predicted by the original and reformulated versions of HFGMC are virtually identical.

For the case of applied transverse tension, the local effective stress, mean stress, and equivalent plastic strain fields have been plotted in figure 5 at an applied global strain level of 0.005 (see fig. 4). As was the case in the global response, figure 5 indicates that the local response predicted by the original and reformulated versions of HFGMC are virtually identical. However, it should be noted that upon close examination of the local fields in figure 5, slight differences between the original and reformulated predictions are discernable. These differences are attributable to small numerical variations that arise due to the distinct inelastic quantities employed in the two formulations. Despite the fact that in both cases, the inelastic terms are approximated using identical Legendre polynomials, these slight differences persist. The reason for this is that in the case of the original formulation of HFGMC, the inelastic terms are derived from stresses and stress moments that have been evaluated in a volume-averaged sense, while in the reformulated version the inelastic terms are computed from surface integrals of the stresses. This directly follows from the Introduction, as the unknowns are the surface integrals of the displacements, see eq. (9) for example. This explanation of the observed differences in figure 5 is confirmed by the fact that prior to yielding, while the material throughout the composite is still in the linear elastic regime, the local and global results predicted by the two formulations are exactly the same.

Table 1.—Constituent material properties.

	E (GPa)	ν	Yield Stress (MPa)
Boron Fiber/Inclusion	413.7	0.20	–
Aluminum Matrix	55.16	0.30	90.

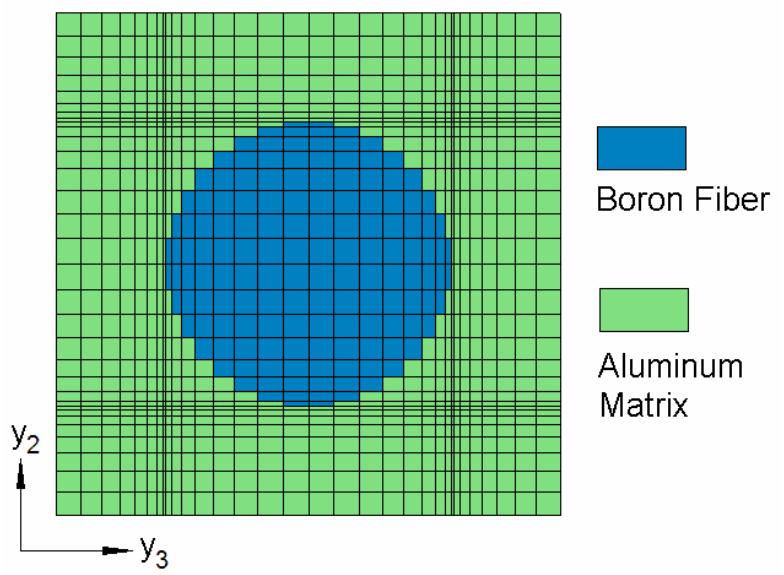

Figure 3.—Doubly-periodic) repeating unit cell, discretized into 32×32 subcells to represent a continuously-reinforced 25% B/Al composite.

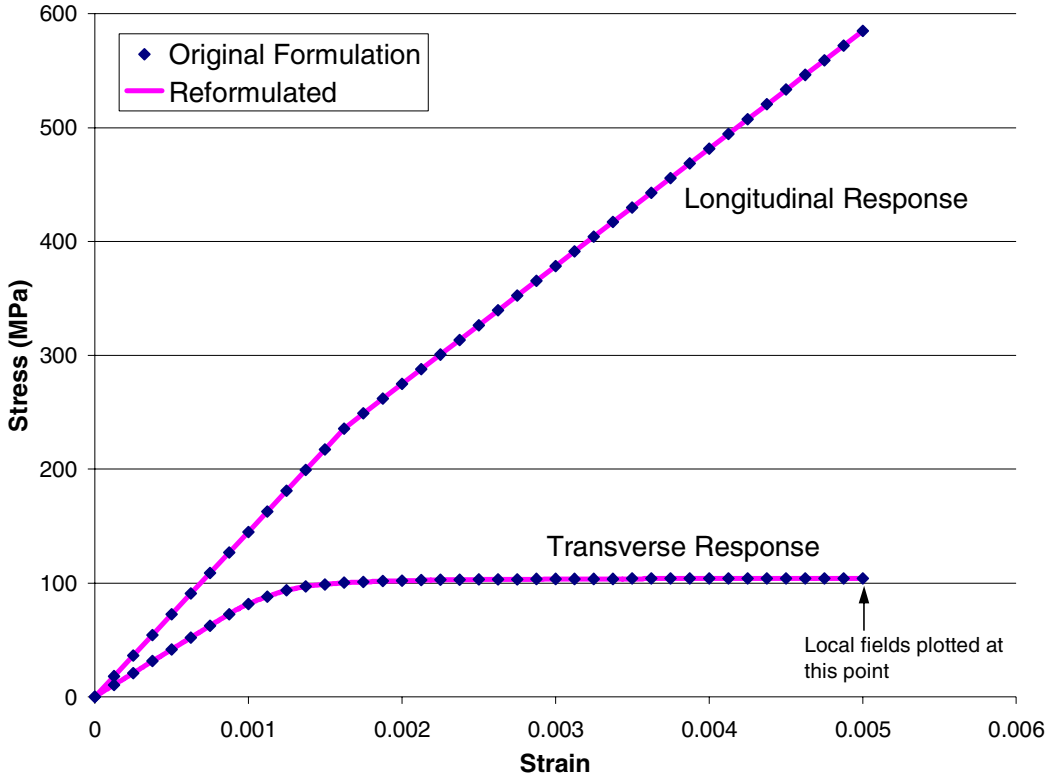

Figure 4.—Global longitudinal and transverse tensile response of 25% continuously reinforced B/Al predicted by the original and reformulated versions of HFGMC.

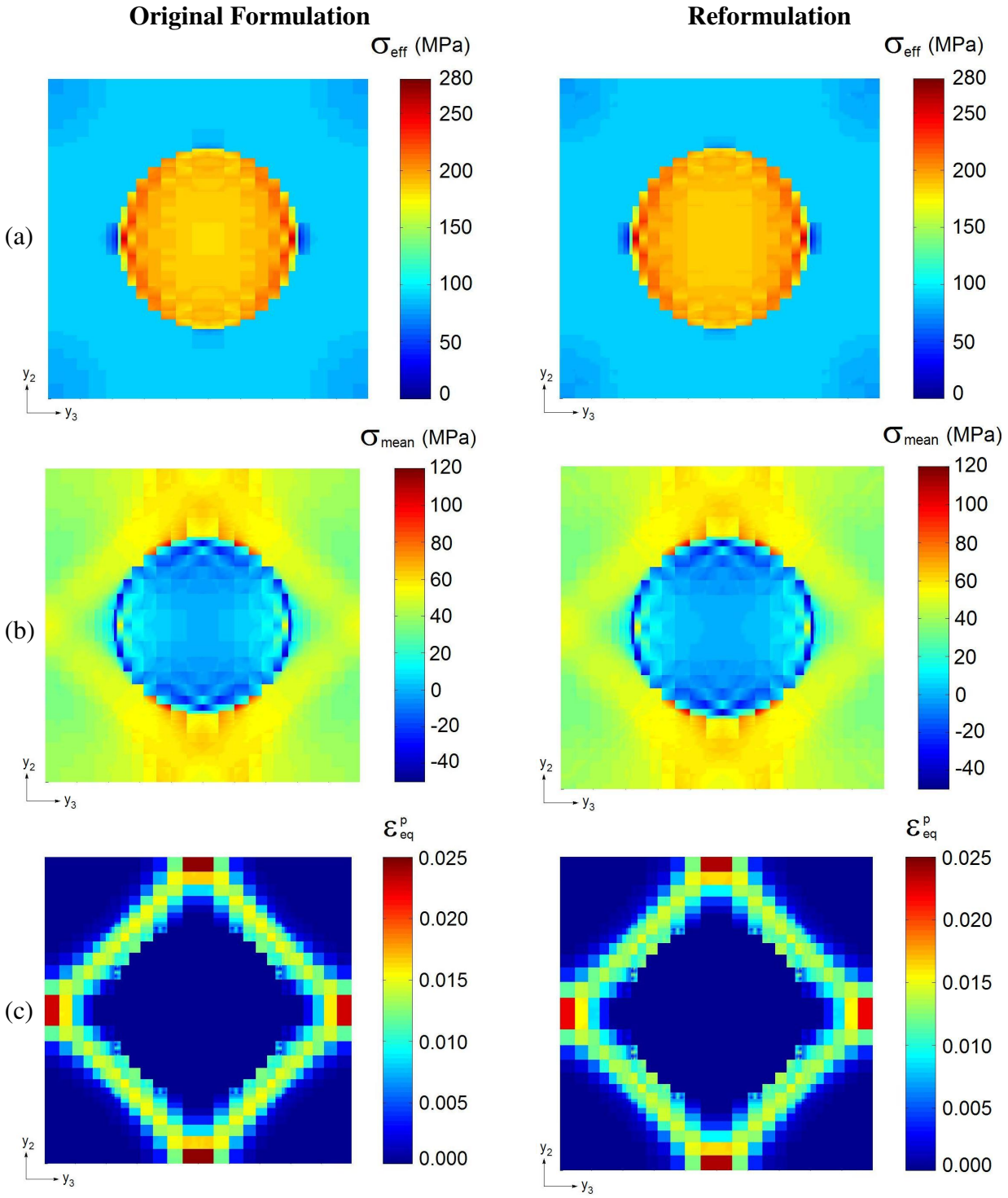

Figure 5.—Local fields predicted by the original and reformulated versions of HFGMC in a 25% B/Al composite. (a) Effective stress, $\sigma_{\text{eff}} = \sqrt{3S_{ij}S_{ij}/2}$, S_{ij} = deviatoric stress components; (b) Mean stress, $\sigma_{\text{mean}} = \left[\sigma_{11} + \sigma_{22} + \sigma_{33}\right]/3$; (c) Equivalent plastic strain, $\varepsilon_{eq}^{p} = \int\sqrt{2d\varepsilon_{ij}^{p}d\varepsilon_{ij}^{p}/3}$.

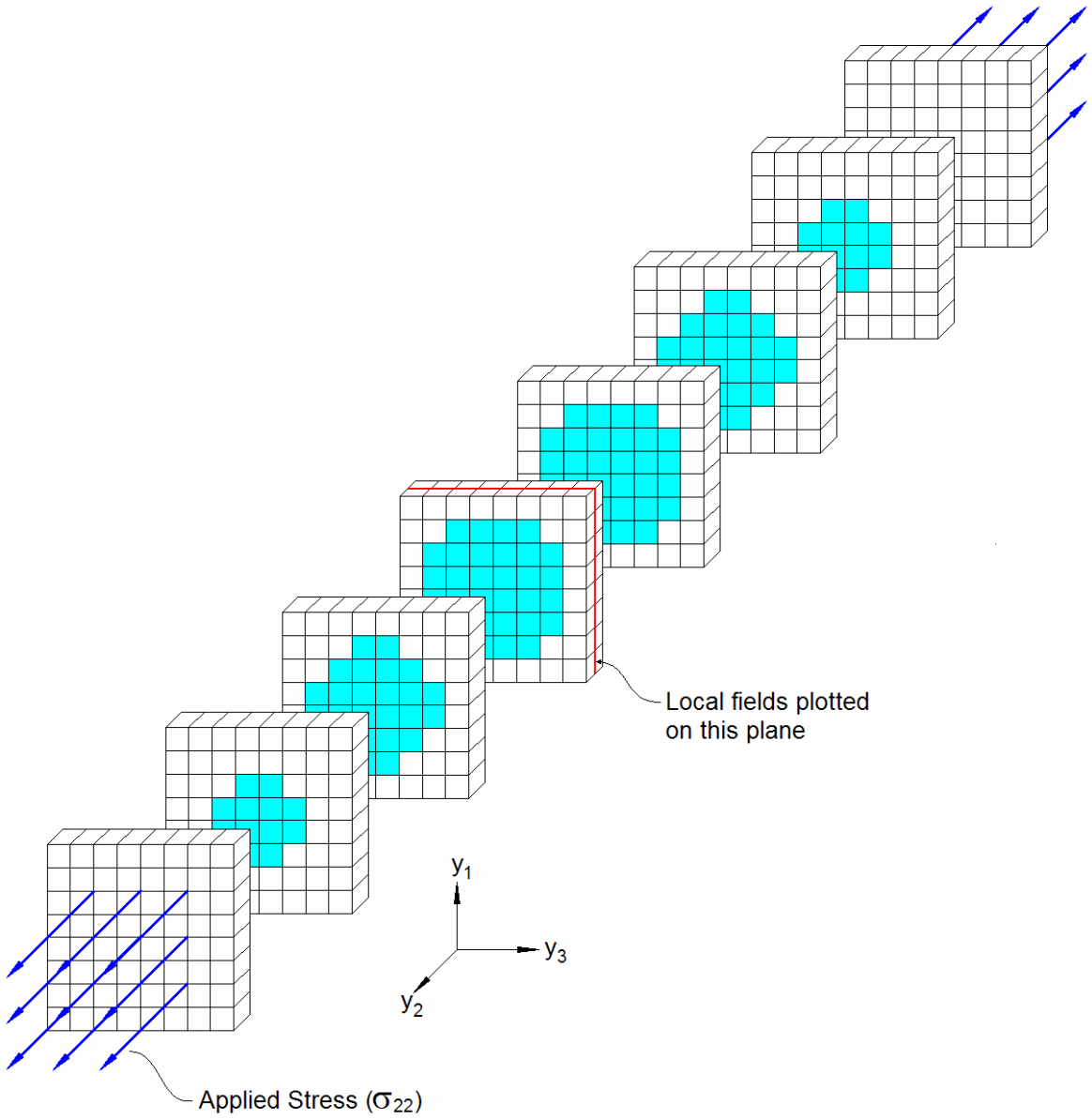

Figure 6.—Exploded view of the triply-periodic repeating unit cell, discretized into 8×8×8 subcells to represent a discontinuously-reinforced 25% B/Al composite.

For the discontinuously-reinforced (i.e., particulate) composite case, the employed RUC is shown in figure 6; where it has been discretized into 8×8×8 subcells in order to approximate a spherical inclusion. This RUC was employed to simulate the tensile response of a 25% particulate reinforced B/Al composite, with both perfect and imperfect (weak) interfacial bonding. In the weak bonding case, the interfacial proportionality constant, $R_j(t)$, was set to a large value, which simulates an extremely compliant interface, for illustrative purposes. The global tensile responses predicted by the original and reformulated versions of HFGMC in the case of perfect and weak bonding are plotted in figure 7. The influence of the weak interfacial bonding is immediately apparent in the predictions; with the perfect bonding case being considerably stiffer and yielding at a much higher global stress as compared with the weakly bonded case. Again, figure 7 indicates that both the original and reformulated versions of HFGMC yield very similar predictions for the global composite response. Note, in the case of weak

bonding, the predictions are virtually identical, whereas a small difference is noticeable in the perfect bonding case. This difference is again attributable to small numerical differences between the volume-averaged inelastic terms (in the case of the original formulation), and the surface-averaged inelastic terms (in the case of the reformulation). In the elastic regime, the predictions of both formulations are identical.

Once again, the local effective stress, mean stress, and equivalent plastic strain fields are plotted in figures 8 and 9, respectively for both the perfectly bonded and weakly bonded cases. These plots represent the local fields at an applied global strain level of 0.005 (see fig. 7) on the plane near the middle of the RUC indicated in figure 6. Comparing figures 8 and 9, the local effects of the weak interfacial bonding are evident. For example, in the case of perfect bonding (fig. 8), the inclusion is able to support a high load/stress level. In contrast, the weakly bonded inclusion (fig. 9) cannot support much load as the weak interface disallows transfer of stress from the matrix to the inclusion. Thus, the inclusion experiences a very low stress level and, as was shown in the global response plotted in figure 7, it becomes ineffective at stiffening the composite. Comparing the local fields predicted by the original and reformulated versions of HFGMC, it is again clear that both formulations yield very similar local results for both perfect and weak interfacial bonding within the particulate reinforced B/Al composite. The slight differences that are discernable are again attributable to numerical differences that arise between the volume-averaged and surface-averaged inelastic terms.

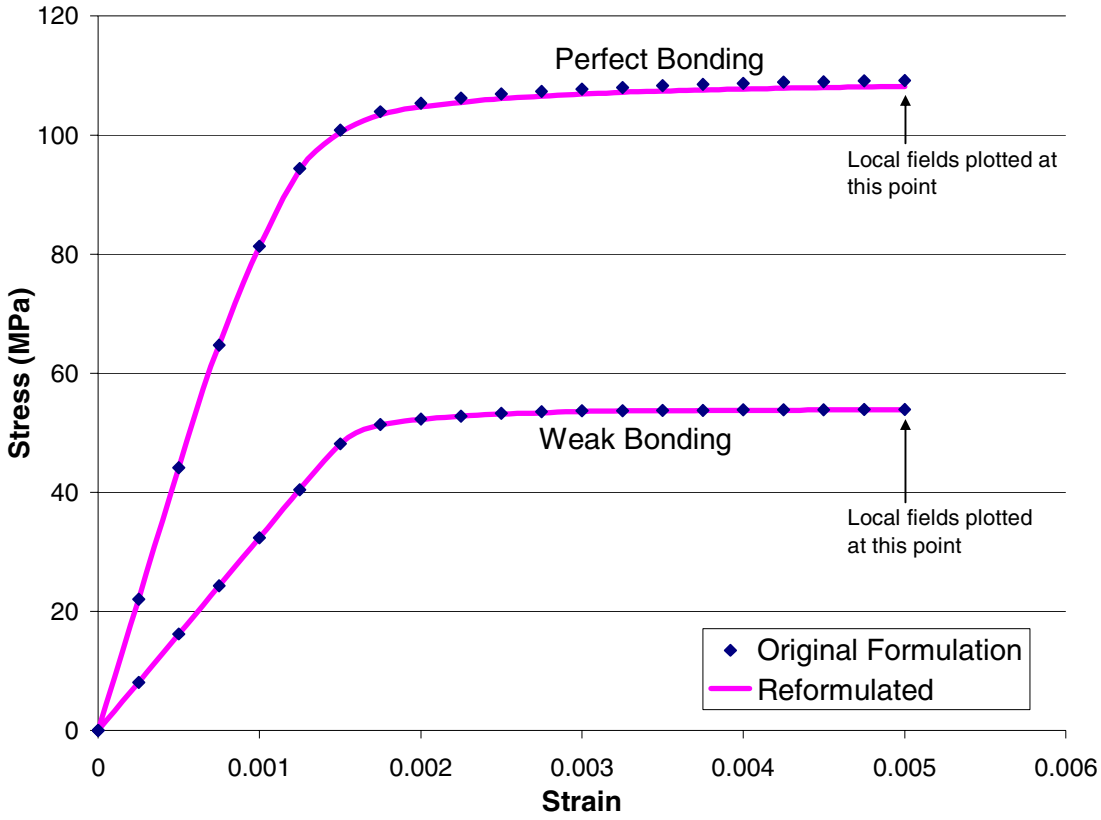

Figure 7.—Global tensile response of 25% discontinuous B/Al predicted by the original and reformulated versions of HFGMC with perfect and weak interfacial bonding.

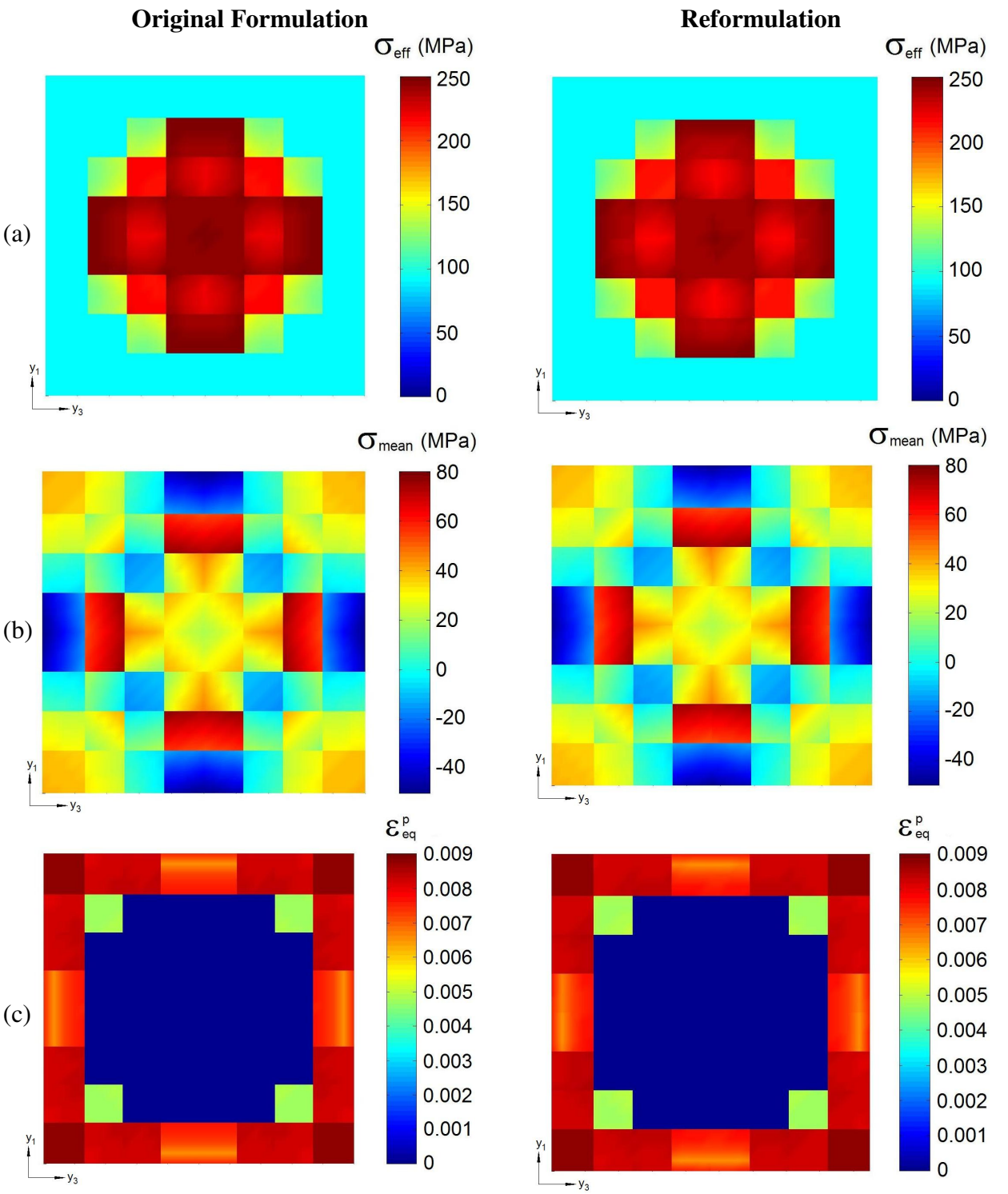

Figure 8.—Local fields predicted by the original and reformulated versions of triply-periodic HFGMC in a 25% discontinuous B/Al composite with **perfect bonding**. (a) Effective stress, $\sigma_{\text{eff}} = \sqrt{3S_{ij}S_{ij}/2}$, S_{ij} = deviatoric stress components; (b) Mean stress, $\sigma_{\text{mean}} = \left[\sigma_{11} + \sigma_{22} + \sigma_{33}\right]/3$; (c) Equivalent plastic strain, $\varepsilon_{eq}^{p} = \int\sqrt{2d\varepsilon_{ij}^{p}d\varepsilon_{ij}^{p}/3}$.

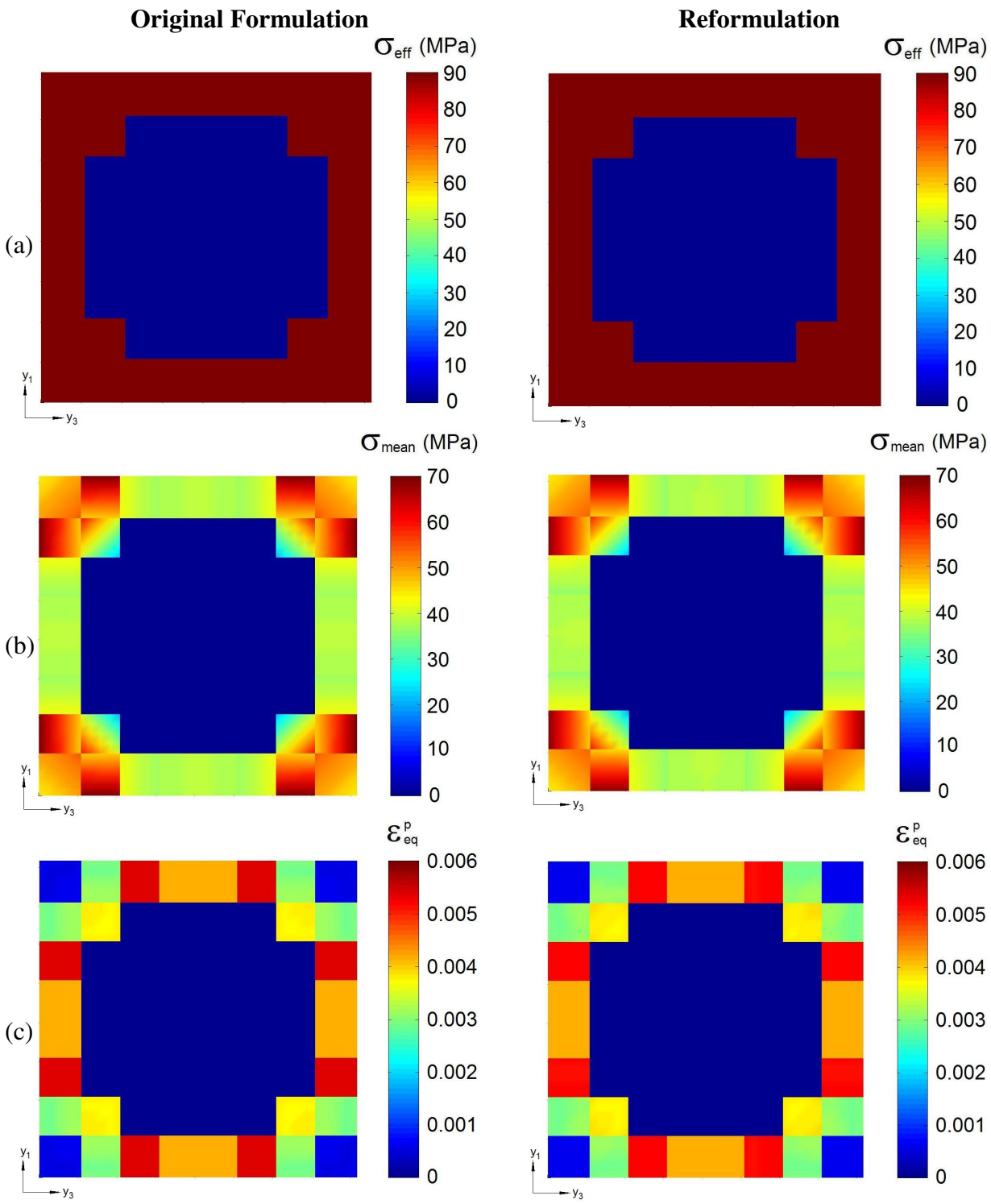

Figure 9.—Local fields predicted by the original and reformulated versions of triply-periodic HFGMC in a 25% discontinuous B/Al composite with **weak bonding**. (a) Effective stress, $\sigma_{\text{eff}} = \sqrt{3S_{ij}S_{ij}/2}$, S_{ij} = deviatoric stress components; (b) Mean stress, $\sigma_{\text{mean}} = \left[\sigma_{11} + \sigma_{22} + \sigma_{33}\right]/3$; (c) Equivalent plastic strain, $\varepsilon^{p}_{eq} = \int\sqrt{2d\varepsilon^{p}_{ij}d\varepsilon^{p}_{ij}/3}$.

The results presented above clearly illustrate the fact that the original and reformulated implementations of the HFGMC theory yield essentially identical results aside from small numerical deviations associated with the inelastic strain approximation methods utilized. Tables 2 and 3 now present a direct comparison of the efficiency of the two formulations as a function of the RUC discretization. In order to isolate the effect of the reduced number of equations offered by the reformulation, these results were generated for the linear elastic case in which only the effective thermo-elastic properties of the composite material are determined. That is, in contrast to the results presented in figures 4 and 7, a full simulation of the elasto-plastic behavior of the composite has not been performed. This eliminates the effects of the incremental loading procedure and the inelasticity iterations on the execution time of the codes, as these effects are not relevant to the improved efficiency offered by the reformulation. Note that these execution time comparison cases were executed on a 1.7 GHz PC with 1 GB of RAM.

Table 2 presents the improved computational efficiency attributable to the reformulation of the continuously reinforced (doubly-periodic) version of HFGMC. The RUC is varied from a simple coarse 4×4 discretization to a well-refined 64×64 discretization. The reformulation decreases the number of equations dramatically and, to a lesser extent, decreases the number of non-zero terms in the matrices $\mathbf{K}$ and $\mathbf{K}'$ (see eqs. (3) and (10)). As a result, the sparseness (i.e., fraction of non-zero terms relative to total number of elements in matrix) decreases in the case of the reformulation. Most importantly, the execution time associated with the reformulated version of HFGMC decreases as compared to the original formulation. For RUCs with only a few subcells, this improvement in execution time is modest (1.4 times, see table 2). However, in the case of the 64×64 representation, the execution time is improved by 2.4 times.

The discontinuously reinforced (triply-periodic) version of HFGMC is considerably more computationally demanding than the doubly-periodic version for both the original formulation and reformulation. Comparing the 8×8 doubly-periodic case (which has 64 subcells) with the (4×4×4) triply-periodic case (which also has 64 subcells), the number of equations increases from 960 to 1344 (in the original formulation) and from 432 to 720 (in the reformulation), see tables 2 and 3. This larger number of equations obviously leads to greater execution time when using the triply-periodic version. In table 3, the RUC discretization is varied from a coarse 4×4×4 representation to a more refined 12×12×12 representation. As was the case in the doubly-periodic version, the number of equations are decreased roughly by a factor of two. The number of non-zero terms in the $\mathbf{K}$ and $\mathbf{K}'$ matrices, however, now increases slightly in the reformulated version of HFGMC. The sparseness of these matrices is again decreased due to the reformulation. Once again, comparing triply periodic execution times for the original and reformulated versions of HFGMC, see table 3, it is clear that the computational efficiency of the reformulation increases significantly as the number of subcells increases. In fact, due to excessive memory solver requirements, solving the 12×12×12 composite property problem proved intractable using the original formulation; whereas the reformulated version successfully determined the solution. For the 10×10×10 discretization, the reformulation was 7.8 times faster than the original formulation.

Table 2.—Comparison of the original and reformulated continuously reinforced (doubly-periodic) HFGMC implementations for determination of effective B/Al thermo-elastic properties as a function of RUC discretization.

RUC	Subcells	Equations		Non-Zeros		Sparseness		Execution Time (s)		Speed Up
		Org.	Reform.	Org.	Reform.	Org.	Reform.	Org.	Reform.	
4x4	16	240	120	1,184	872	0.979	0.939	0.028	0.020	1.4
8x8	64	960	432	5,056	3,728	0.995	0.980	0.074	0.043	1.72
16x16	256	3,840	1,632	20,672	15,008	0.9985	0.9943	0.31	0.21	1.47
32x32	1,024	15,360	6,336	83,392	59,840	0.99964	0.9985	1.81	0.97	1.86
64x64	4,096	61,440	24,960	334,784	238,592	0.999911	0.99961	15.8	6.47	2.44

Table 3.—Comparison of the original and reformulated discontinuously reinforced (triply-periodic) HFGMC implementations for determination of effective B/Al thermo-elastic properties as a function of RUC discretization.

RUC	Subcells	Equations		Non-Zeros		Sparseness		Execution Time (s)		Speed Up
		Org.	Reform.	Org.	Reform.	Org.	Reform.	Org.	Reform.	
4x4x4	64	1344	720	8,688	9,216	0.995	0.982	0.24	0.24	1.0
6x6x6	216	4,536	2,268	30,648	32,100	0.9985	0.9937	5.34	2.52	2.12
8x8x8	512	10,752	5,184	73,872	76,368	0.99936	0.99715	60.1	20.1	2.99
10x10x10	1,000	21,000	9,900	145,560	149,076	0.99967	0.99847	782	99.9	7.89
12x12x12	1,728	36,288	16,848	252,912	257,280	0.99980	0.99909	-	568	<12

4. Conclusion

This paper has presented a comparison of the original formulation and reformulation of the high-fidelity generalized method of cells (HFGMC) micromechanics model for analysis of continuous and discontinuous composite materials. The original formulation of HFGMC (Aboudi et al., 2001, 2002, 2003), employed the microvariables appearing in the theory's assumed quadratic local displacement field (eq. (2)) as the basic unknowns; whereas, recently, Bansal and Pindera (2004) presented a reformulation of the doubly-periodic, linear elastic HFGMC theory wherein the averaged interfacial displacements on the surfaces of the subcells serve as the basic unknowns. This reformulation significantly reduces the number of unknowns and consequently the number of linear algebraic equations that must be solved. As a result, the computational efficiency of HFGMC has been correspondingly enhanced. The present work extends the reformulated HFGMC to the inelastic, weakly-bonded, and triply-periodic cases.

Results presented herein indicate that, aside from some small numerical differences due to different numerical treatments of the inelastic terms in the two formulations, both (original and reformulated) implementations of HFGMC yield identical predictions on both the global (composite) and local (constituent) levels. This was demonstrated for the case of a perfectly bonded, continuously reinforced B/Al composite loaded longitudinally and transversely, as well as a discontinuous (particulate) B/Al composite case with both perfect and weak interfacial bonding.

Finally, a direct comparison of the computational efficiency of the original and reformulated versions of HFGMC was presented as a function of repeating unit cell refinement. Due to the reduced number of unknowns/equations present in the reformulated implementation, the model's execution time has been improved significantly (the limit being approximately an order of magnitude increase) compared to the original formulation. The speed-up associated with the reformulation increases as the RUC density increases (by dividing it into a greater number of subcells). For the continuous reinforcement (doubly-periodic) version, the reformulation provided an execution speed-up of 2.4 times for a 64×64 subcell discretization, while, in the case of discontinuous reinforcements, the reformulation provided an execution speed-up of 7.8 times for a 10×10×10 subcell discretization, over that of the original formulation.

References

Aboudi, J., Generalized Effective Stiffness Theory for the Modeling of Fiber-Reinforced Composites, Int. J. Solids Struct., vol. 17, 1005–1018, 1981.

Aboudi, J., A Continuum Theory for Fiber-Reinforced Elastic Viscoplastic Composites, Int. J. Eng. Sci., vol. 20, 605–621, 1982.

Aboudi, J., Harmonic Waves in Composite Materials. Wave Motion, vol. 8, 289–303, 1986.

Aboudi, J., Transient Waves in Composite Materials. Wave Motion, vol. 9, 141–156, 1987.

Aboudi, J., Wave Propagation in Damaged Composite Materials. Int. J. Solids and Structures, vol. 24, 117–138, 1988.

Aboudi, J., Mechanics of Composite Materials: A Unified Micromechanical Approach, Elsevier, Amsterdam 1991.

Aboudi, J., Micromechanical Analysis of Thermoinelastic Multiphase Short-Fiber Composites, Compos. Eng., vol. 5, 839–850, 1995.

Aboudi, J., Micromechanical Analysis of Composites by the Method of Cells - Update, Appl. Mech. Rev. vol. 49, S83–S91, 1996.

Aboudi, J., Micromechanical Analysis of Fully Coupled Electro-Magneto-Thermo-Elastic Multiphase Composites, Smart Mater. Struct., vol. 10, 867–877, 2001.

Aboudi, J., The Generalized Method of Cells and High-Fidelity Generalized Method of Cells Micromechanical Models - A Review. Mech. Adv. Materl. Struct. 11, 329–366, 2004.

Aboudi, J., Pindera, M.-J., and Arnold, S.M., Higher-Order Theory for Functionally Graded Materials, Composites Part B, vol. 30, 777–832, 1999.

Aboudi, J., Pindera, M.J. and Arnold, S.M., Linear Thermoelastic Higher-Order Theory for Periodic Multiphase Materials, J. Applied Mech., vol. 68, pp. 697–707, 2001.

Aboudi, J., Pindera, M.-J., and Arnold, S.M., High-Fidelity Generalized Method of Cells for Inelastic Periodic Multiphase Materials, NASA/TM—2002-211469, 2002.

Aboudi, J., Pindera, M.-J., and Arnold, S.M., Higher-Order Theory for Periodic Multiphase Materials with Inelastic Phases, Int. J. Plasticity, vol. 19, 805–847, 2003

Bansal Y., and Pindera, M.J., Efficient Reformulation of the Thermoelastic Higher Order Theory for FGMs, NASA CR 2002-211909, 2002.

Bansal, Y. and Pindera, M-J., Efficient Reformulation of the Thermoelastic Higher-Order Theory for Functionally Graded Materials. J. Thermal Stresses, vol. 26, pp. 1055–1092, 2003.

Bansal, Y., and Pindera, M-J, Testing the Predictive Capability of the High-Fidelity Generalized Method of Cells Using an Efficient Reformulation. NASA/CR—2004-213043, 2004.

Bednarcyk, B.A., and Arnold, S.M., A New Local Debonding Model with Application to the Transverse Tensile and Creep Behavior of Continuously Reinforced Titanium Composites. NASA/TM—2000-210029, 2000.

Bednarcyk, B.A., and Arnold, S.M., MAC/GMC 4.0 User's Manual, NASA/TM—2002-212077, 2002a.

Bednarcyk, B.A., and Arnold, S.M., Transverse Tensile and Creep Modeling of Continuously Reinforced Titanium Composites with Local Debonding. Int. J. Solids Struct. vol. 39, 1987–2017, 2002b.

Bednarcyk, B.A., Arnold, S.M., Aboudi, J., and Pindera, M.-J., Local Field Effects in Titanium Matrix Composites Subjected to Fiber-Matrix Debonding. Int. J. Plasticity, vol. 20, 1707–1737, 2004.

Bednarcyk, B.A. and Pindera, M.-J., Inelastic Response of a Woven Carbon/Copper Composite Part II: Micromechanics Model, J. Composite Materials, vol. 34, 299–331, 2000.

Mendelson, A., Plasticity: Theory and Application. Krieger Publishing Co., Malabar, FL, 1986. (reprint edition).

Nemat-Nasser, S., and Hori, M., Micromechanics: Overall Properties of Heterogeneous Materials, North-Holland, Amsterdam, 1999.

Paley, M., and Aboudi, J., Micromechanical Analysis of Composites by the Generalized Cells Model, Mech. Materials, vol. 14, 127–139, 1992.

Pindera, M.-J., and Bednarcyk, B.A., An Efficient Implementation of the Generalized Method of Cells for Unidirectional, Multi-Phased Composites with Complex Microstructures, Composites Part B, vol. 30, 87–105, 1999.

Zhong, Yi. and Pindera, M.J., Efficient Reformulation of HOTFGM: Heat Conduction with Variable Thermal Conductivity, NASA/CR—2002- 211910, 2002.

REPORT DOCUMENTATION PAGE

Form Approved
OMB No. 0704-0188

1. AGENCY USE ONLY (*Leave blank*)	2. REPORT DATE	3. REPORT TYPE AND DATES COVERED
	December 2004	Technical Memorandum

4. TITLE AND SUBTITLE

Comparison of the Computational Efficiency of the Original Versus Reformulated High-Fidelity Generalized Method of Cells

5. FUNDING NUMBERS

WBS–22–714–70–63

6. AUTHOR(S)

Steven M. Arnold, Brett Bednarcyk, and Jacob Aboudi

7. PERFORMING ORGANIZATION NAME(S) AND ADDRESS(ES)

National Aeronautics and Space Administration
John H. Glenn Research Center at Lewis Field
Cleveland, Ohio 44135–3191

8. PERFORMING ORGANIZATION REPORT NUMBER

E–14973

9. SPONSORING/MONITORING AGENCY NAME(S) AND ADDRESS(ES)

National Aeronautics and Space Administration
Washington, DC 20546–0001

10. SPONSORING/MONITORING AGENCY REPORT NUMBER

NASA TM—2004-213438

11. SUPPLEMENTARY NOTES

Steven M. Arnold, NASA Glenn Research Center; Brett Bednarcyk, Ohio Aerospace Institute, Brook Park, Ohio 44142; and Jacob Aboudi, Faculty of Engineering, Tel Aviv University, Ramat Aviv 69978, Israel. Responsible person, Steven M. Arnold, organization code RSL, 216–433–3334.

12a. DISTRIBUTION/AVAILABILITY STATEMENT

Unclassified - Unlimited
Subject Categories: 24 and 39 Distribution: Nonstandard

Available electronically at http://gltrs.grc.nasa.gov

This publication is available from the NASA Center for AeroSpace Information, 301–621–0390.

12b. DISTRIBUTION CODE

13. ABSTRACT ***(Maximum 200 words)***

The High-Fidelity Generalized Method of Cells (HFGMC) micromechanics model has recently been reformulated by Bansal and Pindera (in the context of elastic phases with perfect bonding) to maximize its computational efficiency. This reformulated version of HFGMC has now been extended to include both inelastic phases and imperfect fiber-matrix bonding. The present paper presents an overview of the HFGMC theory in both its original and reformulated forms and a comparison of the results of the two implementations. The objective is to establish the correlation between the two HFGMC formulations and document the improved efficiency offered by the reformulation. The results compare the macro and micro scale predictions of the continuous reinforcement (doubly-periodic) and discontinuous reinforcement (triply-periodic) versions of both formulations into the inelastic regime, and, in the case of the discontinuous reinforcement version, with both perfect and weak interfacial bonding. The results demonstrate that identical predictions are obtained using either the original or reformulated implementations of HFGMC aside from small numerical differences in the inelastic regime due to the different implementation schemes used for the inelastic terms present in the two formulations. Finally, a direct comparison of execution times is presented for the original formulation and reformulation code implementations. It is shown that as the discretization employed in representing the composite repeating unit cell becomes increasingly refined (requiring a larger number of sub-volumes), the reformulated implementation becomes significantly (approximately an order of magnitude at best) more computationally efficient in both the continuous reinforcement (doubly-periodic) and discontinuous reinforcement (triply-periodic) cases.

14. SUBJECT TERMS

Micromechanics; Elastic; Inelastic; Computational; Deformation; Composites; Analysis

15. NUMBER OF PAGES

25

16. PRICE CODE

17. SECURITY CLASSIFICATION OF REPORT	18. SECURITY CLASSIFICATION OF THIS PAGE	19. SECURITY CLASSIFICATION OF ABSTRACT	20. LIMITATION OF ABSTRACT
Unclassified	Unclassified	Unclassified	